Akademie věd České republiky
Ústav teorie informace a automatizace, v.v.i.

Academy of Sciences of the Czech Republic
Institute of Information Theory and Automation

RESEARCH REPORT

Eva Lainová, Lenka Kuklišová Pavelková, Ladislav Jirsa

Approximate Bayesian state estimation and output prediction using state-space model with uniform noise

No. 2381 December 2019

GAČR 18-15970S

ÚTIA AV ČR, P.O.Box 18, 182 08 Prague, Czech Republic
Tel: (+420)266052422, Fax: (+420)286890378, Url: http://www.utia.cas.cz, E-mail: utia@utia.cas.cz

Any opinions and conclusions expressed in this report are those of the author and do not necessarily represent the views of the institute.

Contents

Abstract
This paper contributes to the problem of approximate Bayesian state estimation and output prediction using state space model with uniformly distributed noise. Algorithms for Bayesian filtering and output prediction for states uniformly distributed on an orthotopic support and Bayesian filtering and output prediction for states uniformly distributed on a parallelotopic support are presented and compared.

Keywords: Bayesian filtering, state estimation, output prediction, uniform noise, parallelotopic support, orthotopic support

1 Introduction

A linear stochastic state space model is often used as a model that provides prediction of the system behaviour. For problems, such as fault detection, robust-model predictive control, feedback control, where system states are unmeasurable and either states or outputs, or both are constrained to particular sets, Bayesian filters are a fitting tool for the state estimation.

The purpose of this technical paper is to summarize algorithms for estimation of states using state space model with noise uniformly distributed on an orthotopic support and for estimation of states using state space model with noise uniformly distributed on a parallelotopic support. The other main task is to summarize output prediction for a state space model with noise uniformly distributed on an orthotopic support and to introduce an algorithm for output prediction for a state space model with noise uniformly distributed on a parallelotopic support and to compare both algorithms for state estimation and output prediction and to provide the results.

Throughout the paper following notation is used. Capital letters A are appointed to matrices. Vectors and scalars are in lower case b. The length of vector z is represented by ℓ_z. A_{ij} is the element of matrix A in the i-th row and j-th column. A_i denotes the i-th row of matrix A. The symbol $f(\cdot \mid \cdot)$ denotes a conditional probability density function (pdf). $\propto$ means equality up to a constant factor.

2 Multidimensional uniform distribution and its support

In this section, the uniform pdf is defined and examples of its supports are introduced. Geometrical characteristics of the pdf supports are described.

2.1 Definition of uniform pdf

Let the characteristic function $\chi(z)$ on set Z be defined as

$$\chi(z) = \begin{cases} 1 & \text{for} \quad z \in Z, \\ 0 & \text{otherwise.} \end{cases}$$

Let $z \in \mathbb{R}^n$ and $Vz : \mathbb{R}^n \to \mathbb{R}^k$ be a continuous linear mapping. Let $Z = \{z : a \leq Vz \leq b\}$, where a, $b \in \mathbb{R}^k$, V is a $k \times n$, $k \geq n$ matrix of rank n. The characteristic function $\chi(z)$ on set Z can be equivalently defined as $\chi(z) = \chi(a \leq Vz \leq b)$.

Let uniform pdf $\mathcal{U}_z(a \leq Vz \leq b)$ of a random variable z be defined as a product of the characteristic function $\chi(z)$ on Z and a normalising constant K

$$\mathcal{U}_z(a \leq Vz \leq b) = K\chi(a \leq Vz \leq b). \tag{1}$$

The normalising constant can be omitted using notation

$$\mathcal{U}_z(a \leq Vz \leq b) \propto \chi(a \leq Vz \leq b).$$

Note that the set Z is called the support of $\mathcal{U}_z$. In the paper, following equivalent notation for uniform pdf is used

$$\mathcal{U}_z(a \leq Vz \leq b) = \mathcal{U}_z(a, b, V).$$

If V is the identity matrix, i.e. $V = I$,

$$\mathcal{U}_z(a \leq z \leq b) = \mathcal{U}_z(a, b).$$

2.2 Examples of supports of the uniform pdf

Support of the uniform pdf defined in (1) can be a complex set depending on the dimension of V. Let V be a $k \times n$, $k \geq n$ matrix of rank n, so that the volume $\mathcal{V}$ of the set Z is finite. Volume $\mathcal{V}$ of the pdf support Z is equal to K^{-1}, i.e. $\mathcal{V} = K^{-1}$, where K is the normalising constant from (1) The support Z is a convex set bounded by a finite number of faces.

A convex polytope is defined as a convex set bounded by a finite number of flat faces. *A zonotope* Z_Z is a special case of convex polytope which can be expressed as

$$Z_Z = \{z : a \leq Vz \leq b\}, \tag{2}$$

where upper and lower bounds a, b are vectors of length k, V is a matrix of size $k \times l_z$ and rank ℓ_z. Zonotope is an intersection of $k \geq l_z$ strips S. Each strip is defined as

$$Z_{S_i} = \{z : a_i \leq Vz_i \leq b_i\}, \tag{3}$$

where $i = 1, \ldots, l_z$.

A parallelotope Z_P is a special case of zonotope (3), where $k = l_z$ i.e. a, b are vectors of length ℓ_z, V is an invertible square matrix of size $\ell_z \times \ell_z$. Equivalently to (2), parallelotope can be expressed in other forms. For further use, two forms are introduced. The $[-\mathbf{1}, \mathbf{1}]$ form

$$Z_P = \{z : -\mathbf{1}_{(l_z)} \leq Wz - c \leq \mathbf{1}_{(l_z)}\}, \tag{4}$$

where $\mathbf{1}_{(l_z)}$ is unit vector of length ℓ_z. W and c are defined as

$$W_{ij} = \frac{2V_{ij}}{b_i - a_i}, \qquad c_i = \frac{b_i + a_i}{b_i - a_i}. \tag{5}$$

Form (4) can be transformed to form (2) using $a = c - \mathbf{1}_{(l_z)}$, $b = c + \mathbf{1}_{(l_z)}$ and $V = W$.

Applying the knowledge that W as well as V are invertible square matrices of size $\ell_z \times \ell_z$, centroid $\hat{z}$ of the parallelotope expressed in (2) and in (4) can be computed as

$$\hat{z} = Tc, \tag{6}$$

where $T = W^{-1}$. Having found the centroid $\hat{z}$, the parallelotope can be expressed in its centroid form

$$Z_P = \{z : z = \hat{z} + T\xi\}, \tag{7}$$

where $\forall \xi$ s.t. $\|\xi\|_\infty = \max_i(\xi_i) < 1$.

An orthotope Z_O is a special case of parallelotope in (2), where $V = I$, I denotes an identity matrix. Lower and upper bounds $a = \underline{z}$ and $b = \overline{z}$

$$Z_O = \{z : \underline{z} \leq z \leq \overline{z}\}. \tag{8}$$

An orthotope can be also expressed in forms (4) and (7) using $V = I$.

After defining both the parallelotope and the orthotope in multiple forms, volume of both objects can be computed.

Volume computation:

- Computation of a general form of a polytope volume $\mathcal{V}$ is a complex task [6] unnecessary for the purposes of this paper.
- The volume of a zonotope $\mathcal{V}_Z$ is the sum of the $\mathcal{V}_P$ of its generating parallelotopes, see [1].
- Parallelotope

$$\mathcal{V}_P = \mid \det V \mid \prod_{i=1}^{l_z} (b_i - a_i) \tag{9}$$

- Orthotope

$$\mathcal{V}_O = \prod_{i=1}^{l_z} (\overline{z}_i - \underline{z}_i) \tag{10}$$

3 State estimation and output prediction

In the considered Bayesian setup [3], the system is modelled by the following pdfs.

$$\begin{aligned} \text{prior pdf:} \quad & f(x_1) \\ \text{observation model:} \quad & f(y_t \mid x_t) \\ \text{time evolution model:} \quad & f(x_{t+1} \mid x_t, u_t) \end{aligned} \tag{11}$$

where x_t is an unobservable ℓ_x-dimensional system state, y_t is a scalar observable output, u_t is known optional system input and t represents time step, $t \in T$.

It is assumed that system states x_t satisfy Markov property and no direct relationship exists between system inputs and outputs in the observation model in (11). The system inputs consist of a known sequence $u_1, \ldots, u_{\bar{t}}$, where $\bar{t}$ is final time step.

Bayesian state estimation or filtering [3] consists in the evolution of the posterior pdf $f(x_t \mid d(t))$ where $d(t)$ is a sequence of observed data records $d(t) = (y_t, u_t)$, $t \in T$. The evolution of $f(x_t \mid d(t))$ is described by a two-step recursion that starts from the prior pdf $f(x_1)$ and ends by data update at the final time $\bar{t}$.

Data update

$$f(x_t \mid d(t)) = \frac{f(y_t \mid x_t) f(x_t \mid d(t-1))}{\int_{x_t^*} f(y_t \mid x_t) f(x_t \mid d(t-1)) \mathrm{d}x_t} = \frac{f(y_t \mid x_t) f(x_t \mid d(t-1))}{f(y_t \mid d(t-1))} \tag{12}$$

Time update

$$f(x_{t+1} \mid d(t)) = \int_{x_t^*} f(x_{t+1} \mid u_t, x_t) f(x_t \mid d(t)) \mathrm{d}x_t \tag{13}$$

Linear state space model with uniform noise is defined as

$$\begin{aligned} x_t &= Ax_{t-1} + Bu_{t-1} + \nu_t, \quad && \nu_t \sim \mathcal{U}_\nu(-\rho, \rho), \\ y_t &= Cx_t + n_t, && n_t \sim \mathcal{U}_n(-r, r), \end{aligned} \tag{14}$$

where A, B, C are the known model matrices of appropriate dimensions, ν_t is a state noise $\nu_t \in (-\rho, \rho)$ where ρ in a known parameter. n_t represents output noise $n_t \in (-r, r)$ where r in a known parameter.

For further use, an equivalent pdf definition of the linear state space model with uniform noise is presented

$$\begin{aligned} f(x_{t+1} \mid x_t, u_t) &= \mathcal{U}_x(Ax_t + Bu_t - \rho, Ax_t + Bu_t + \rho), \\ f(y_t \mid x_t) &= \mathcal{U}_y(Cx_t - r, Cx_t + r). \end{aligned} \tag{15}$$

3.1 Bayesian filtering and output prediction using state-space model with uniform noise on an orthotopic support (LSUO)

Approximate data update: Data update (12) processes the pdf $f(y_t \mid x_t)$ of the observation model (15) together with the pdf $f(x_t \mid d(t-1))$ which results from previous time update (13). The recursion starts at the time $t = 1$ with the prior pdf $f(x_1)$ (11) which is uniform on an orthotopic support i.e.

$$f(x_1) = \mathcal{U}_{x_1}(\underline{x}_1, \overline{x}_1). \tag{16}$$

Performing the data update according to [8], a posterior pdf $f(x_t \mid d(t))$ with zonotopic support is obtained. This zonotope results from the intersection of an orthotope given by the previous time update or in the first time step by prior pdf $f(x_1)$ and strips given by the new data

$$\begin{aligned} f(x_t \mid d(t)) \propto & \chi(\underline{m}_t - \rho \leq x_t \leq \overline{m}_t + \rho) \times \chi(Cx_t - r \leq y_t \leq Cx_t + r) = \\ = & \chi\left(\begin{bmatrix} \underline{m}_t - \rho \\ y_t - r \end{bmatrix} \leq \begin{bmatrix} I \\ C \end{bmatrix} x_t \leq \begin{bmatrix} \overline{m}_t + \rho \\ y_t + r \end{bmatrix} \right), \end{aligned} \tag{17}$$

where I is an identity matrix of size $\ell_x \times \ell_x$, $\underline{m}_t$ and $\overline{m}_t$ are computed as follows

$$\begin{aligned} \underline{m}_{t;i} &= \sum_{j=1}^{n} \min(A_{ij}\underline{x}_{t-1;j} + B_i u_{t-1}, A_{ij}\overline{x}_{t-1;j} + B_i u_{t-1}), \\ \overline{m}_{t;i} &= \sum_{j=1}^{n} \max(A_{ij}\underline{x}_{t-1;j} + B_i u_{t-1}, A_{ij}\overline{x}_{t-1;j} + B_i u_{t-1}). \end{aligned} \tag{18}$$

The resulting polytopic support is circumscribed by a parallelotope as described in [8]

$$f(x_t \mid d(t)) \approx K_t \chi(\underline{x}_t \leq M_t x_t \leq \bar{\bar{x}}_t). \tag{19}$$

To obtain the required bounds $\underline{x}_t$ and $\overline{x}_t$ another circumscription is necessary. The computation details of circumscribing parallelotope by an orthotope are to be found in [8]. The result is

$$\underline{x}_t \leq x_t \leq \overline{x}_t. \tag{20}$$

The approximate pdf has the form

$$f(x_t \mid d(t)) \approx \mathcal{U}_x(\underline{x}_t, \overline{x}_t). \tag{21}$$

The state point estimate $\hat{x}_t$ is the centre of orthotope

$$\hat{x}_t = \frac{\underline{x}_t + \bar{x}_t}{2}. \tag{22}$$

Approximate time update: The time update (13) processes the pdf $f(x_{t+1} \mid x_t, u_t)$ of time evolution model from (15) and the result of previous data update $f(x_t \mid d(t))$. The time update exactly computed in [8] results with the pdf $f(x_{t+1} \mid d(t))$ having a linear piecewise shape. The original trapezoidal pdf is approximated by a uniform distribution by minimising the Kullback-Leibler divergence of two pdfs [8]. The resulting approximation has the form

$$f(x_{t+1} \mid d(t)) \approx \mathcal{U}_x(\underline{m}_{t+1} - \rho, \overline{m}_{t+1} + \rho). \tag{23}$$

Predictive pdf

Assume output y_t be a scalar. The denominator in (12) represents the Bayesian output predictor

$$f(y_t \mid d(t-1)) = \int_{x_t^*} f(y_t \mid x_t) f(x_t \mid d(t-1)) \mathrm{d}x_t. \tag{24}$$

The predictive pdf of linear state space model with uniform noise with orthotopic support

$$f(y_t \mid d(t-1)) = \int_{x_t^*} \chi(Cx_t - r \leq y_t \leq Cx_t + r) \chi(\underline{m}_t - \rho \leq x_t \leq \overline{m}_t + \rho) \mathrm{d}x_t. \tag{25}$$

According to [2] the approximate pdf of the orthotopic predictor has the form

$$f(y_t \mid d(t-1)) \approx \frac{\chi(\underline{y}_t \leq y_t \leq \overline{y}_t)}{\overline{y}_t - \underline{y}_t}, \tag{26}$$

where

$$\begin{aligned} \underline{y}_t &= C\underline{s} - r, \\ \overline{y}_t &= C\overline{s} + r, \end{aligned} \tag{27}$$

$\underline{s}$ and $\overline{s}$ defined so that

$$\begin{aligned} \underline{s}_i &= \underline{m}_{t;i} - \rho_i, \quad \overline{s}_i = \overline{m}_{t;i} + \rho_i, \qquad \text{if } C_i \geq 0, \\ \underline{s}_i &= \overline{m}_{t;i} + \rho_i, \quad \overline{s}_i = \underline{m}_{t;i} - \rho_i, \qquad \text{if } C_i < 0. \end{aligned} \tag{28}$$

Using algebraic adjustments, the form (27) can be transformed into an equivalent form comparable with the bounds computation for predicted pdf for states uniformly distributed on a parallelotopic support described in the following section. The boundary values $\underline{y}_t$ and $\overline{y}_t$ are then computed as

$$\underline{y}_t = C\hat{x}_t - \left(r+ \mid C \mid \left[\frac{\overline{m}_t - \underline{m}_t}{2} + \rho \right] \right), \tag{29}$$

$$\overline{y}_t = C\hat{x}_t + \left(r+ \mid C \mid \left[\frac{\overline{m}_t - \underline{m}_t}{2} + \rho \right] \right), \tag{30}$$

where $\hat{x}_t = A\hat{x}_{t-1} + Bu_{t-1}$ and $\mid C \mid$ is absolute value by items.

The output point prediction $\hat{y}_t$ is computed as mean value of $f(y_t \mid d(t-1))$

$$\hat{y}_t = \mathrm{E}[y_t \mid d(t-1)] = \frac{\overline{y}_t + \underline{y}_t}{2} = C\left(\frac{\overline{m}_t + \underline{m}_t}{2} \right) = C\mathrm{E}[x_t \mid d(t-1)]. \tag{31}$$

3.2 Bayesian filtering and output prediction using state-space model with uniform noise on a parallelotopic support (LSUP)

Approximate data update: Data update is similar to the data update in LSUO. The pdf $f(x_t \mid d(t-1))$ which results from previous time update (13) is processed with the pdf $f(y_t \mid x_t)$ of the observation model (15). The recursion starts at the time $t = 1$ with the prior pdf $f(x_1)$ (11) which is uniform on parallelotopic support i.e.

$$f(x_1) = \mathcal{U}_{x_1}(a_1, b_1, M_1). \tag{32}$$

According to [3] performing the data update, a posterior pdf $f(x_t \mid d(t))$ with zonotopic support is obtained. This zonotope results from the intersection of a parallelotope given by the previous time update or in the first time step by prior pdf $f(x_1)$ and strips given by the new data

$$\begin{aligned} f(x_t \mid d(t)) \propto & \chi(a_t \leq M_t x_t \leq b_t) \times \chi(Cx_t - r \leq y_t \leq Cx_t + r) \propto \\ \propto & \chi\left(\begin{bmatrix} a_t \\ y_t - r \end{bmatrix} \leq \begin{bmatrix} M_t \\ C \end{bmatrix} x_t \leq \begin{bmatrix} b_t \\ y_t + r \end{bmatrix}\right). \end{aligned} \tag{33}$$

The exact data update (33) is approximated by a pdf uniformly distributed on a parallelotopic support. For details see [3] and [9].

$$f(x_t \mid d(t)) \approx \mathcal{U}_x(a_t, b_t, M_t). \tag{34}$$

The state point estimate $\hat{x}_t$ is the centre of the parallelotopic support of $f(x_t \mid d(t))$. To compute the centre of a parallelotope, the parallelotope needs to be circumscibed by an orthotope using the same approach as in (21). The state point estimate is then computed as

$$\hat{x}_t = \frac{\underline{x}_t + \bar{x}_t}{2}. \tag{35}$$

Approximate time update: The time update (13) processes the pdf $f(x_{t+1} \mid x_t, u_t)$ of time evolution model from (15) and the result of previous data update $f(x_t \mid d(t))$. According to [3], the exact pdf $f(x_{t+1} \mid d(t))$ in non-uniformly distributed on a zonotopic support. It has a linear piecewise shape with parameters a_t, b_t, ρ. The approximation described in [3] leads to $f(x_{t+1} \mid d(t))$ being uniformly distributed on a parallelotopic support

$$f(x_{t+1} \mid d(t)) \approx \mathcal{U}_x(a_{t+1}, b_{t+1}, M_{t+1}). \tag{36}$$

Predictive pdf

Assume, again, output y_t be a scalar. To derive the output predictor of Bayesian filtering for states distributed on a parallelotopic support described in [3]

$$f(y_t \mid d(t-1)) \propto \int_{x_t^*} \chi(Cx_t - r \leq y_t \leq Cx_t + r) \times \chi(a_t \leq Vx_t \leq b_t) \mathrm{d}x_t. \tag{37}$$

The form (37) can be easily transformed into

$$f(y_t \mid d(t-1)) \propto \int_{x_t^*} \chi(-r \leq y_t - Cx_t \leq r) \times \chi(a_t \leq Vx_t \leq b_t) \mathrm{d}x_t \tag{38}$$

and subsequently considering $x_t = [x_{t;1} \dots x_{t;l_x}]'$ following formula is derived.

$$f(y_t \mid d(t-1)) \propto \int \chi\left(y_t - r \leq \sum_{i=1}^{l_x} C_i x_{t;i} \leq y_t + r\right) \times \prod_{j=1}^{l_x} \chi(a_{t;j} \leq \sum_{i=1}^{l_x} V_{ji} x_{t;i} \leq b_{t;j}) \mathrm{d}x_{t;1} \dots \mathrm{d}x_{t;l_x}. \tag{39}$$

The above derived integral (39) contains inequalities and therefore the computation process would need to be split into several branches depending on whether $C_i < 0$ or $C_i \geq 0$ and whether $V_{ji} < 0$ or $V_{ji} \geq 0$. To avoid a complex and long integration process a different approach was chosen.

The first term in (38) represents a strip in the state space. The variable y_t determines the position of the strip with respect to the parallelotope described by the second term in (38). The integral (38) computes the volume of the intersection of the strip and the parallelotope, value of witch depends on variable y_t. Hence where the strip and the parallelotope intersect the value of the integral (38) is non zero otherwise its value is zero.

The strip given by the first term in (38) shifts across the parallelotope given by the second term in (38) by changing y_t. The resulting predictive pdf $f(y_t \mid d(t-1))$ is a function of y_t and has a trapezoidal shape. The trapezoidal pdf is approximated by a uniform pdf.

According to [8] the way to achieve optimal approximation in Bayesian sense is to approximate the trapezoidal $f(y_t \mid d(t-1))$ by a uniform pdf on the support of $f(y_t \mid d(t-1))$.

The resulting uniform approximation of the predictive pdf has the form

$$f(y_t \mid d(t-1)) \approx \frac{\chi(\underline{y}_t \leq y_t \leq \overline{y}_t)}{\overline{y}_t - \underline{y}_t}. \tag{40}$$

The boundary values $\underline{y}_t$ and $\overline{y}_t$ are computed using the approach described in [9]. Described intersection between strip given by the first term in (38) and parallelotope given by the second term in (38) can be expressed as

$$1 = \frac{1}{r} C\hat{x}_t - \frac{\underline{y}_t}{r} - \frac{1}{r} \sum_{i=1}^{l_x} CT_{i;t}, \tag{41}$$

$$-1 = \frac{1}{r} C\hat{x}_t - \frac{\overline{y}_t}{r} + \frac{1}{r} \sum_{i=1}^{l_x} CT_{i;t}, \tag{42}$$

which can easily be transformed into

$$\underline{y}_t = C\hat{x}_t - \left(r + \sum_{i=1}^{l_x} CT_{i;t} \right), \tag{43}$$

$$\overline{y}_t = C\hat{x}_t + \left(r + \sum_{i=1}^{l_x} CT_{i;t} \right), \tag{44}$$

where $\hat{x}_t$ is the centre of the parallelotope given by the second term in (38) computed according to (6).

The output point prediction $\hat{y}_t$ is computed as mean value of $f(y_t \mid d(t-1))$

$$\hat{y}_t = \mathrm{E}[y_t \mid d(t-1)] = \frac{\overline{y}_t + \underline{y}_t}{2}. \tag{45}$$

3.3 Algorithmic summary

Here, recursive algorithms for state estimation and output prediction described in this section are summarised. Is is assumed that model matrices A, B, C as well as noise bounds ρ, r are known.

LSUO

Initialisation:

- Choose final time $\bar{t} > 0$, set initial time $t = 1$
- Set values $\underline{x}_1$, $\overline{x}_1$ of the prior pdf (16) and u_1

On-line:

1. Set $t = t + 1$
2. Compute $\underline{m}_t$, $\overline{m}_t$ in (18)
3. Compute predictive pdf according to (26)
4. Get the point output predictor $\hat{y}_t$ (31)
5. Perform data update according to (17)
6. Approximate $f(x_t \mid d(t))$ from (17) to obtain form (19) for details see [8]
7. Compute the state estimates bounds $\underline{x}_t$ and $\overline{x}_t$ as described in [8] to obtain the resulting form (21)
8. Compute the state point estimate $\hat{x}_t$ (22)
9. If $t < \bar{t}$, go to 1., if $t = \bar{t}$ the recursion ends

LSUP

Initialisation:

- Choose final time $\bar{t} > 0$, set initial time $t = 1$
- Set values a_1, b_1, M_1 of the prior pdf (32) and u_1

On-line:

1. Set $t = t + 1$
2. Compute a_t, b_t, M_t according to (33)
3. Compute predictive pdf according to (40)
4. Get the point output predictor $\hat{y}_t$ (45)
5. Perform data update as described in [3]
6. Approximate $f(x_t \mid d(t))$ to obtain form (34) for details see [3]
7. Compute the state point estimate $\hat{x}_t$ (35)
8. If $t < \bar{t}$, go to 1., if $t = \bar{t}$ the recursion ends

4 Experiments

In this section, the previously described algorithms for state estimation and output prediction are compared on multiple systems (sets of model (14) matrices A, B, C).

4.1 Experiment setup

Following systems of known linear coefficients A, B, C from the state space model (14) are used to demonstrate the proposed algorithms properties.

System S_1 from [2]

$$A = \begin{bmatrix} 0.4 & -0.3 & 0.1 \\ -0.4 & 0.4 & 0 \\ 0.3 & 0.2 & 0.1 \end{bmatrix}, \quad B = \begin{bmatrix} 0.1 \\ 0.6 \\ 0.3 \end{bmatrix}, \quad C = \begin{bmatrix} -1 & 0.9 & -0.5 \end{bmatrix} \tag{46}$$

Position-velocity system S_2 from [3]

$$A = \begin{bmatrix} 1 & 1 \\ 0 & 1 \end{bmatrix}, \quad B = \begin{bmatrix} 0 \\ 0 \end{bmatrix}, \quad C = \begin{bmatrix} 1 & 0 \end{bmatrix} \tag{47}$$

System S_3 from [7]

$$A = \begin{bmatrix} 0.8144 & -0.0905 \\ 0.0905 & 0.9953 \end{bmatrix}, \quad B = \begin{bmatrix} 0.0905 \\ 0.0047 \end{bmatrix}, \quad C = \begin{bmatrix} 0 & 1 \end{bmatrix} \tag{48}$$

Input u_t is randomly generated as $u_t \sim \mathcal{N}(0, 1)$. Length of data sequences is $\bar{t} = 500$. The experiment results of both algorithms (LSUO and LSUP) were obtained using Monte Carlo method. Each experiment was run 100 times. The reported results are the average of the 100 Monte Carlo runs.

As performance measures, the following criteria are used.

Total norm-squared error (TNSE)

$$\text{TNSE} = \sum_{t=1}^{\bar{t}} \sum_{j=1}^{\ell_z} (\hat{z}_{t;j} - z_{t;j})^2, \quad z \in \{x, y\}. \tag{49}$$

- T_1-TNSE of states estimation LSUO (49)
- T_2-TNSE of states estimation LSUP (49)

- T_3-TNSE of output prediction LSUO (49)
- T_4-TNSE of output prediction LSUP (49)
- V_1-volume of state pdf support LSUO (10)
- V_2-volume of state pdf support LSUP (9)
- L_1-length of predictive pdf support LSUO
- L_2-length of predictive pdf support LSUP
- P_1-number of simulated states outside estimated bounds LSUO (in %)
- P_2-number of simulated states outside estimated bounds LSUP (in %)
- P_3-number of simulated outputs outside predicted bounds LSUO (in %)
- P_4-number of simulated outputs outside predicted bounds LSUP (in %)
- P_5-number of state pdf support volumes (LSUP) smaller than corresponding state support volumes (LSUO) (in %)
- P_6-number of predictive pdf support volumes (LSUP) smaller than corresponding predictive pdf support volumes (LSUO) (in %)
- P_7-number of state pdf supports (LSUP) fully nested inside corresponding state supports (LSUO) (in %)
- P_8-number of predictive pdf supports (LSUP) fully nested inside corresponding predictive pdf supports (LSUO) (in %)
- P_9-average percentage of state pdf support (LSUP) lying inside corresponding state support (LSUO) (in %)
- P_{10}-average percentage of predictive pdf support (LSUP) lying inside corresponding predictive pdf support (LSUO) (in %)

4.2 Results for system S_1

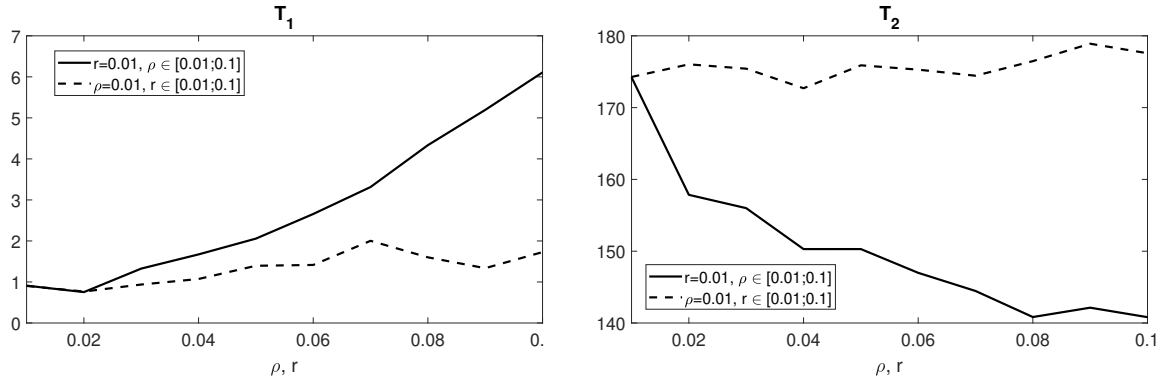

Figure 1: TNSE of states estimation LSUO (left) and LSUP (right) for system S_1 (46) depending on state noise parameter ρ and output noise parameter r.

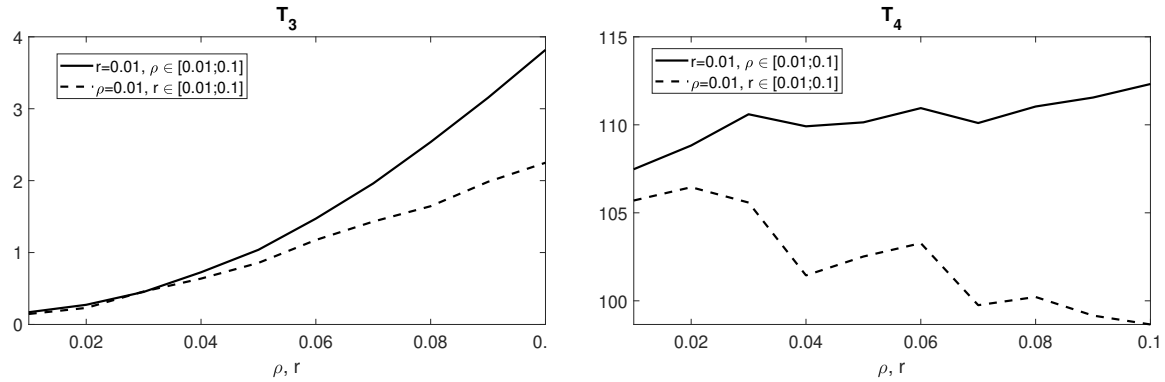

Figure 2: TNSE of output prediction LSUO (left) and LSUP (right) for system S_1 (46) depending on state noise parameter ρ and output noise parameter r.

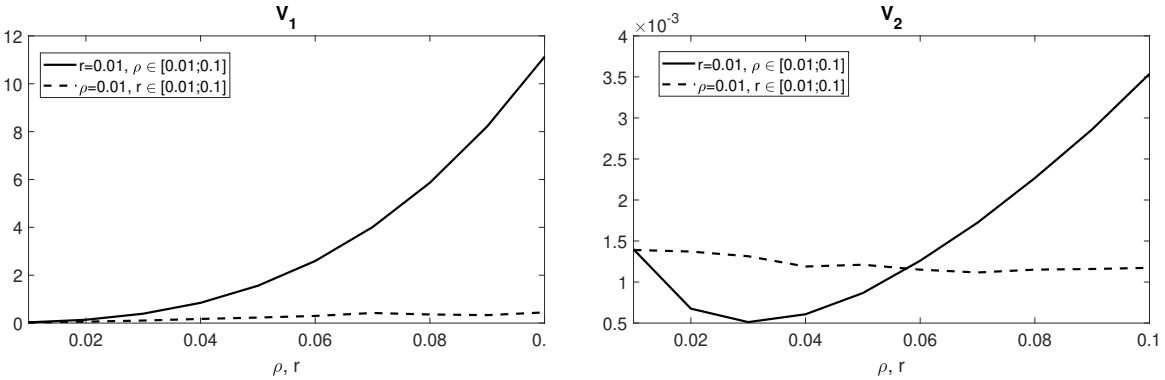

Figure 3: Volume of state pdf support LSUO (left) and LSUP (right) for system S_1 (46) depending on state noise parameter ρ and output noise parameter r.

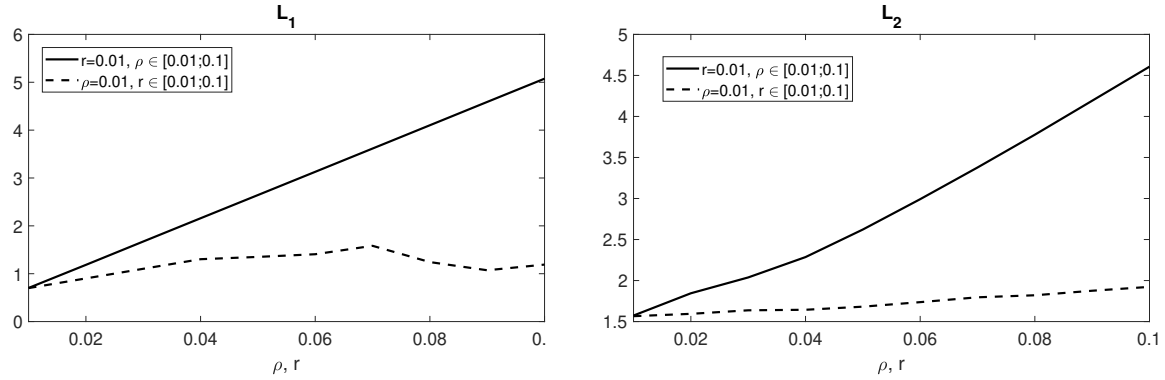

Figure 4: Length of state pdf support estimation LSUO (left) and LSUP (right) for system S_1 (46) depending on state noise parameter ρ and output noise parameter r.

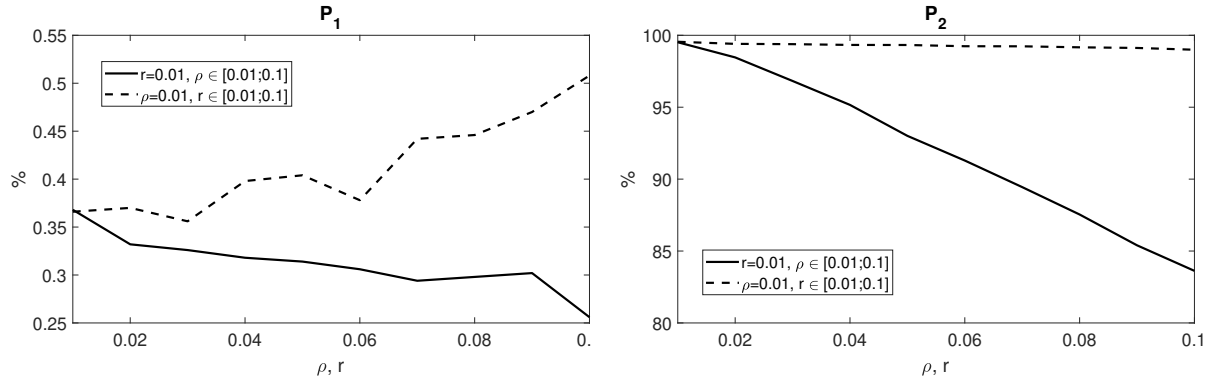

Figure 5: Number of simulated states outside estimated bounds LSUO (left) and LSUP (right)for system S_1 (46) depending on state noise parameter ρ and output noise parameter r.

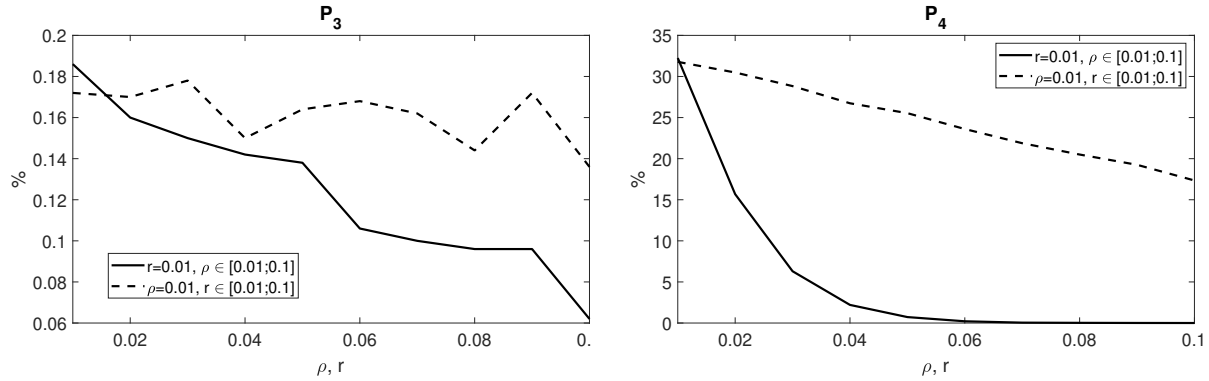

Figure 6: Number of simulated outputs outside estimated bounds LSUO (left) and LSUP (right) for system S_1 (46) depending on state noise parameter ρ and output noise parameter r.

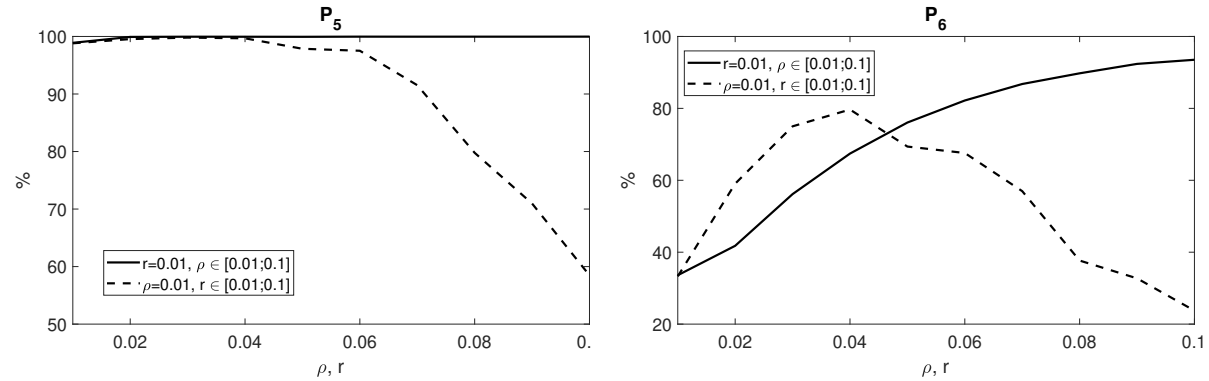

Figure 7: Number of state (left) and predictive (right) pdf support volumes (LSUP) smaller than corresponding support volumes (LSUO) for system S_1 (46) depending on state noise parameter ρ and output noise parameter r.

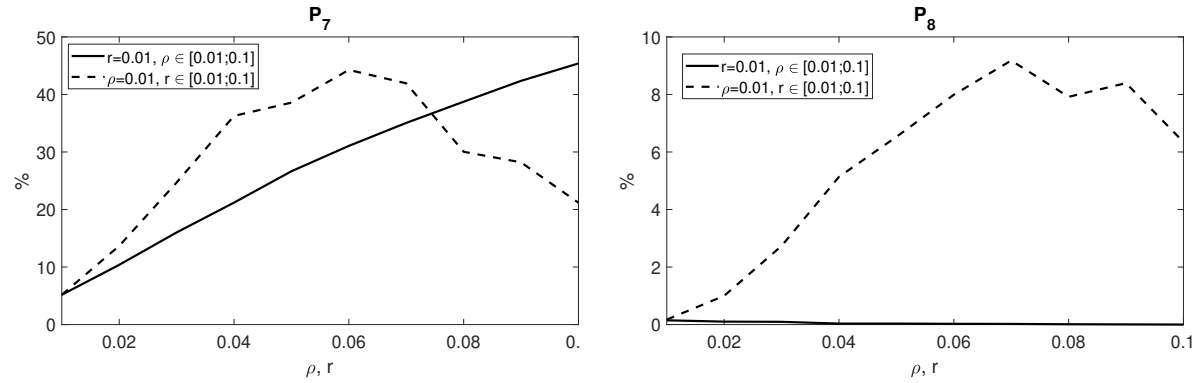

Figure 8: Number of state (left) and predictive (right) pdf supports (LSUP) fully nested inside corresponding supports (LSUO) for system S_1 (46) depending on state noise parameter ρ and output noise parameter r.

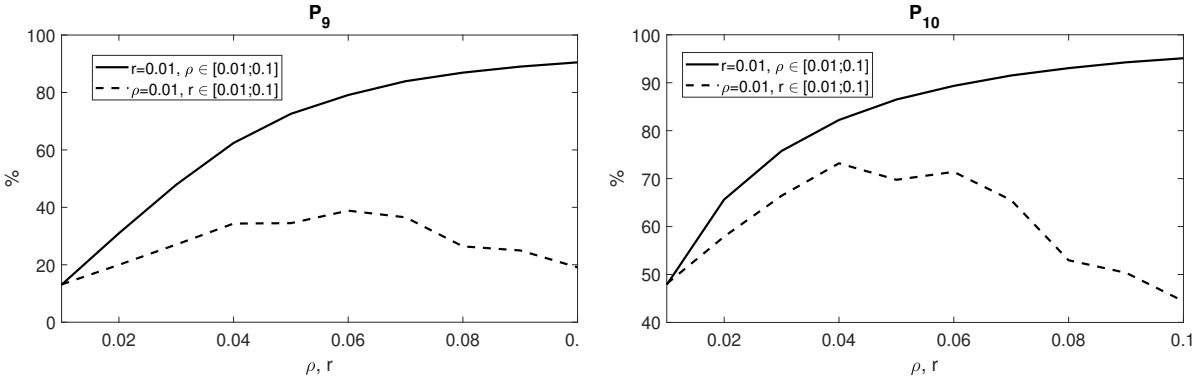

Figure 9: Average percentage of state (left) and predictive (right) pdf support (LSUP) lying inside corresponding support (LSUO) for system S_1 (46) depending on state noise parameter ρ and output noise parameter r.

4.3 Results for system S_2

Graphs for criteria P_1,P_3 and P_4 are not presented because the number of simulated states outside estimated bounds using algorithm LSUO and the number of simulated outputs outside predicted bounds using algorithm LSUO as well as using algorithm LSUP for the setting of parameters $\rho \in [0.01, 0.1]$ and $r \in [0.01, 0.1]$ is zero. This means for system S_2 (47) no simulated states lie outside estimated bounds using LSUO and no simulated outputs lie outside predicted bounds.

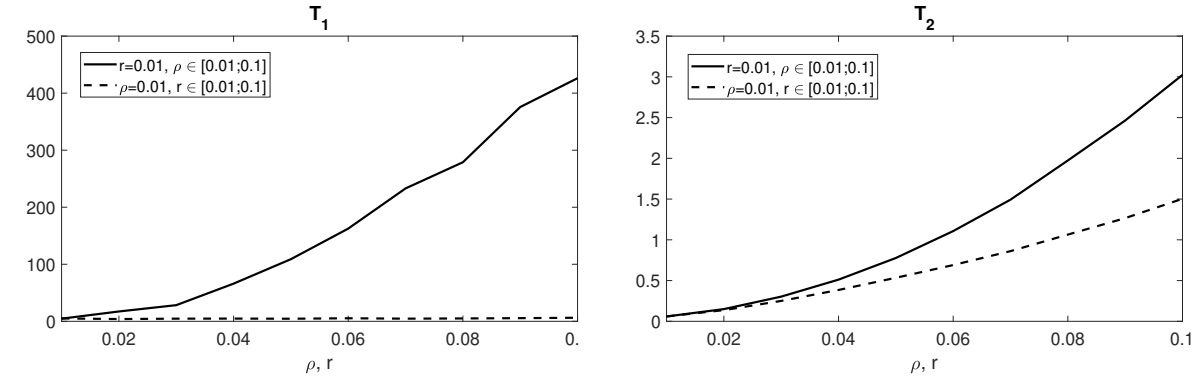

Figure 10: TNSE of states estimation LSUO (left) and LSUP (right) for system S_2 (47) depending on state noise parameter ρ and output noise parameter r.

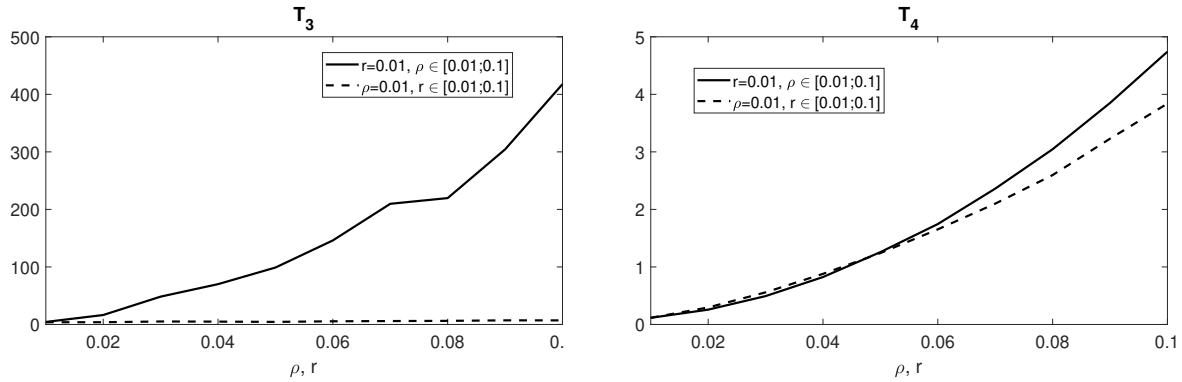

Figure 11: TNSE of output prediction LSUO (left) and LSUP (right) for system S_2 (47) depending on state noise parameter ρ and output noise parameter r.

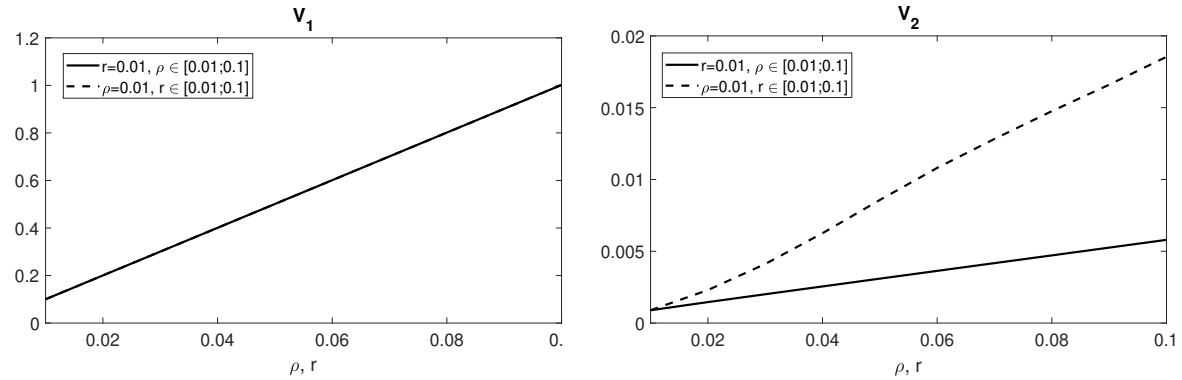

Figure 12: Volume of state pdf support estimation LSUO (left) and LSUP (right) for system S_2 (47) depending on state noise parameter ρ and output noise parameter r.

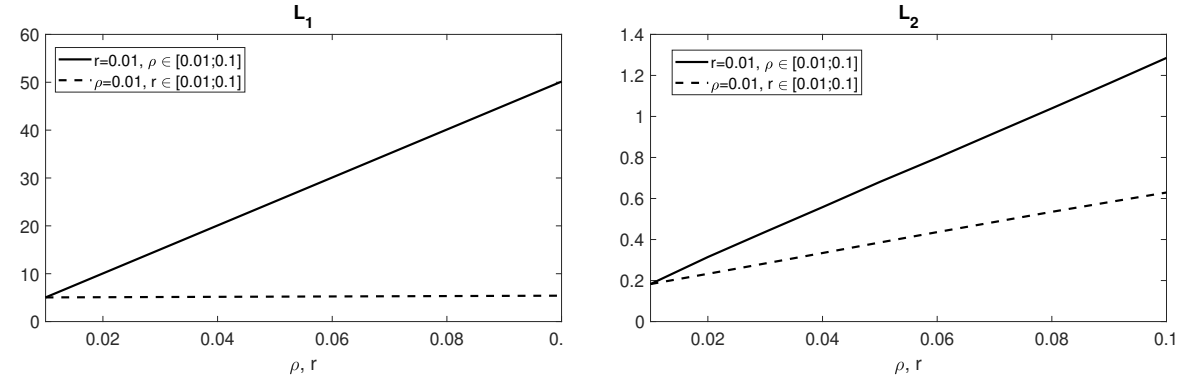

Figure 13: Length of state pdf support estimation LSUO (left) and LSUP (right) for system S_2 (47) depending on state noise parameter ρ and output noise parameter r.

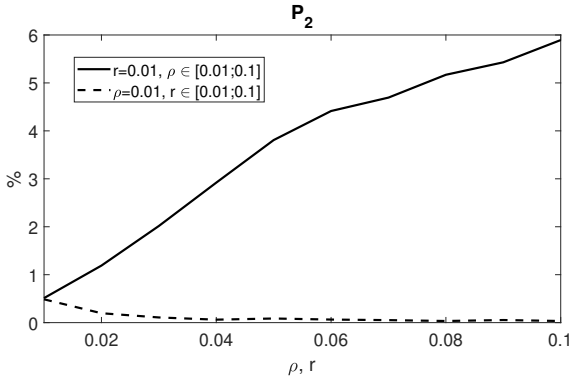

Figure 14: Number of simulated states outside estimated bounds LSUO (left) and LSUP (right) for system S_2 (47) depending on state noise parameter ρ and output noise parameter r.

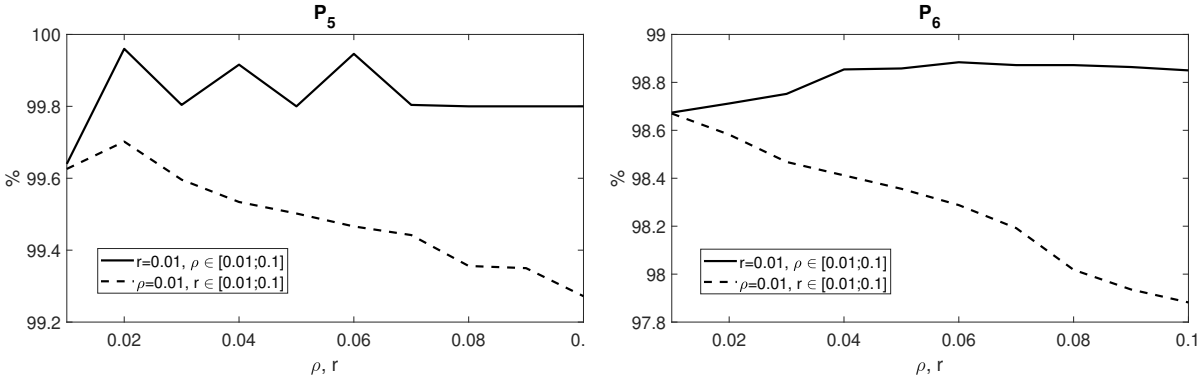

Figure 15: Number of state (left) and predictive (right) pdf support volumes (LSUP) smaller than corresponding support volumes (LSUO) for system S_2 (47) depending on state noise parameter ρ and output noise parameter r.

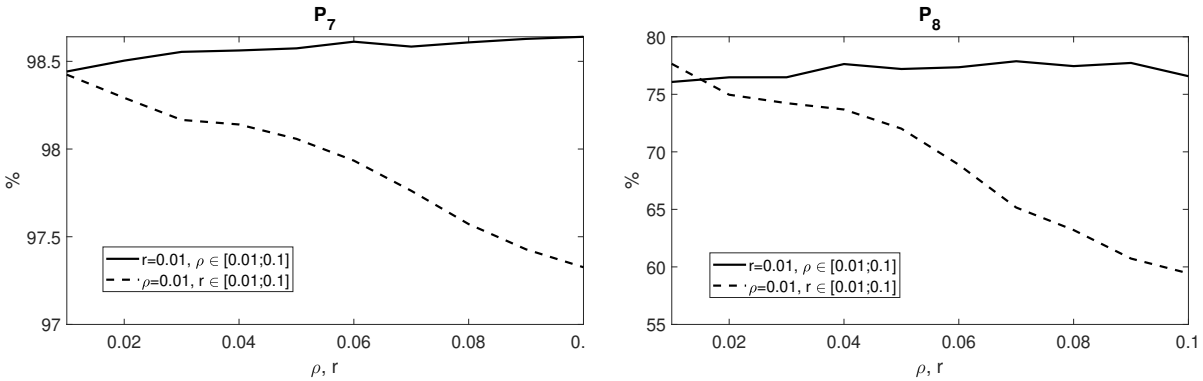

Figure 16: Number of state (left) and predictive (right) pdf supports (LSUP) fully nested inside corresponding supports (LSUO) for system S_2 (47) depending on state noise parameter ρ and output noise parameter r.

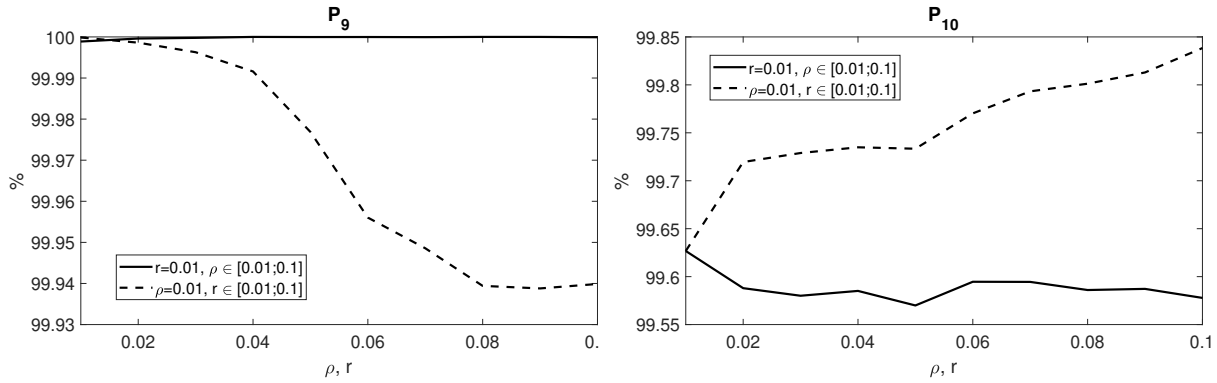

Figure 17: Average percentage of state (left) and predictive (right) pdf support (LSUP) lying inside corresponding support (LSUO) for system S_2 (47) depending on state noise parameter ρ and output noise parameter r.

4.4 Results for system S_3

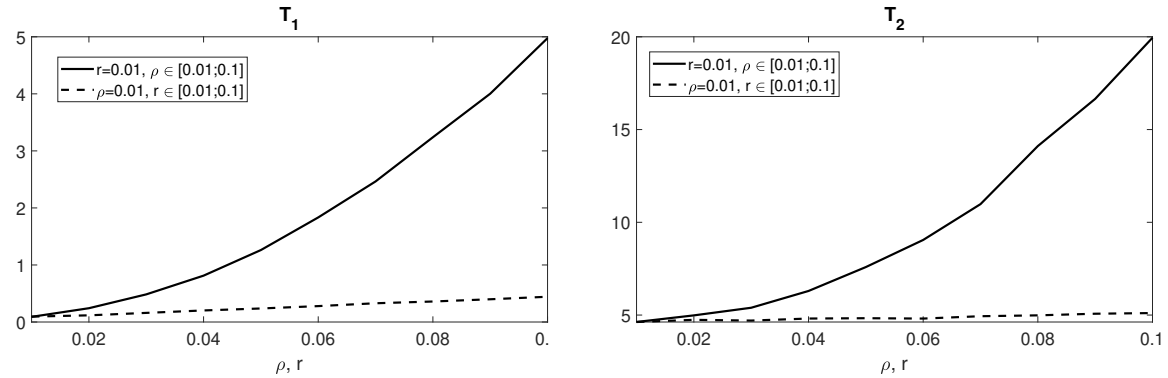

Figure 18: TNSE of states estimation LSUO (left) and LSUP (right) for system S_3 (48) depending on state noise parameter ρ and output noise parameter r.

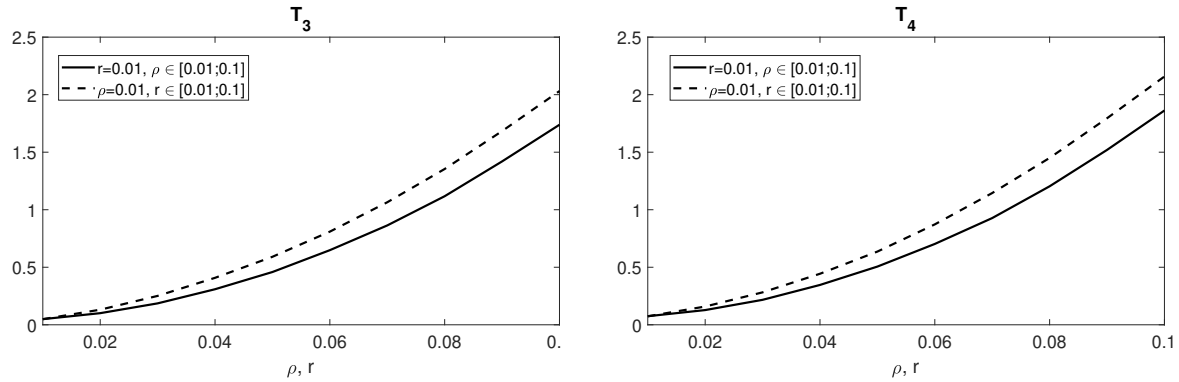

Figure 19: TNSE of output prediction LSUO (left) and LSUP (right) for system S_3 (48) depending on state noise parameter ρ and output noise parameter r.

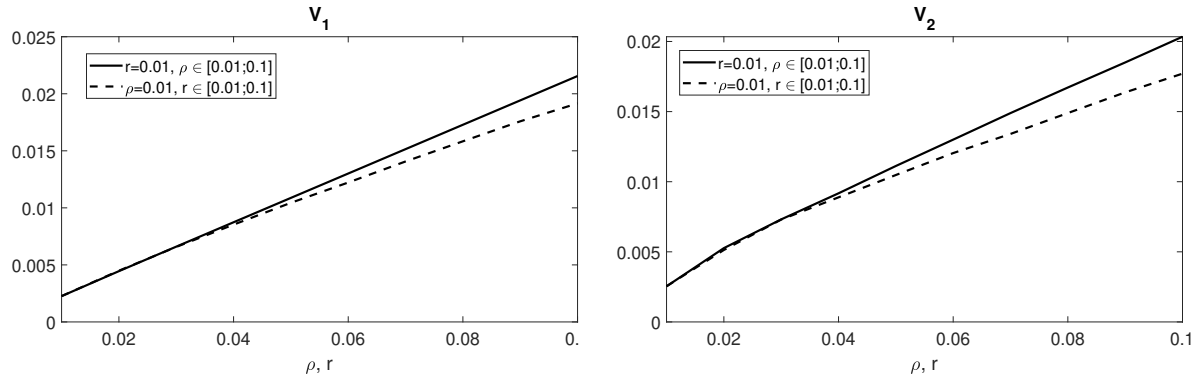

Figure 20: Volume of state pdf support LSUO (left) and LSUP (right) for system S_3 (48) depending on state noise parameter ρ and output noise parameter r.

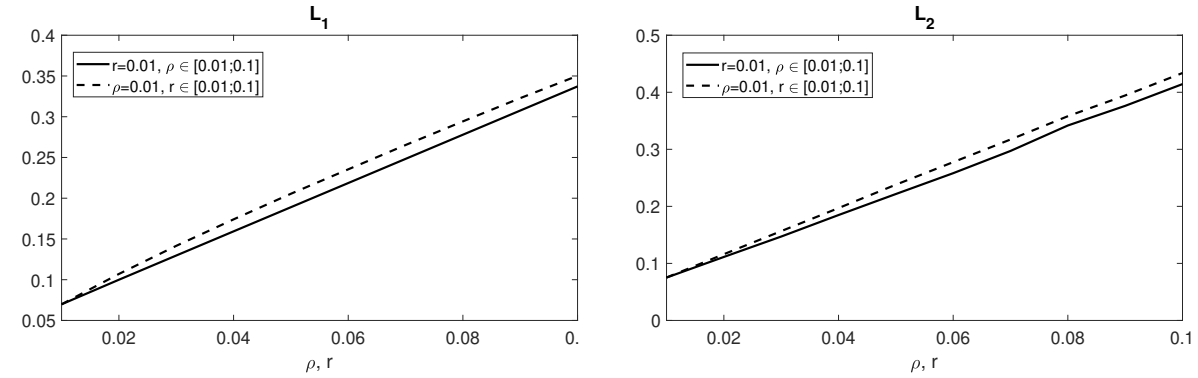

Figure 21: Length of predictive pdf support LSUO (left) and LSUP (right) for system S_3 (48) depending on state noise parameter ρ and output noise parameter r.

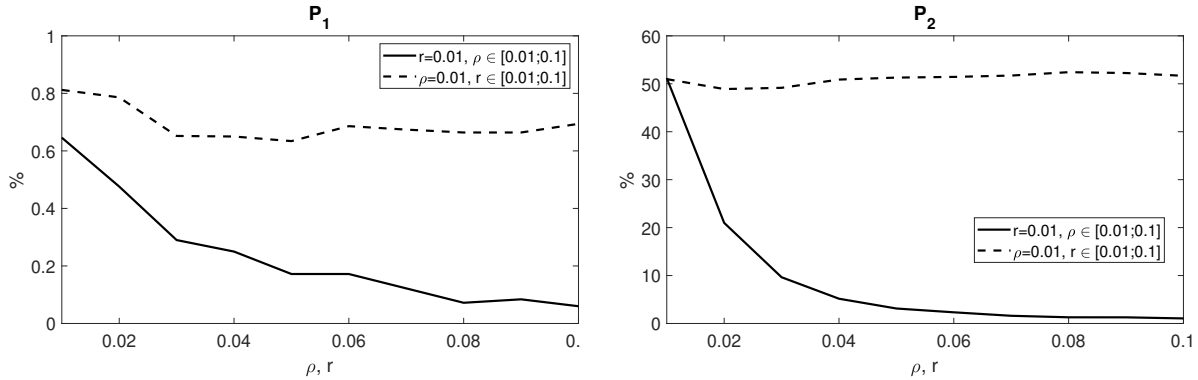

Figure 22: Number of simulated states outside estimated bounds LSUO (left) and LSUP (right) for system S_3 (48) depending on state noise parameter ρ and output noise parameter r.

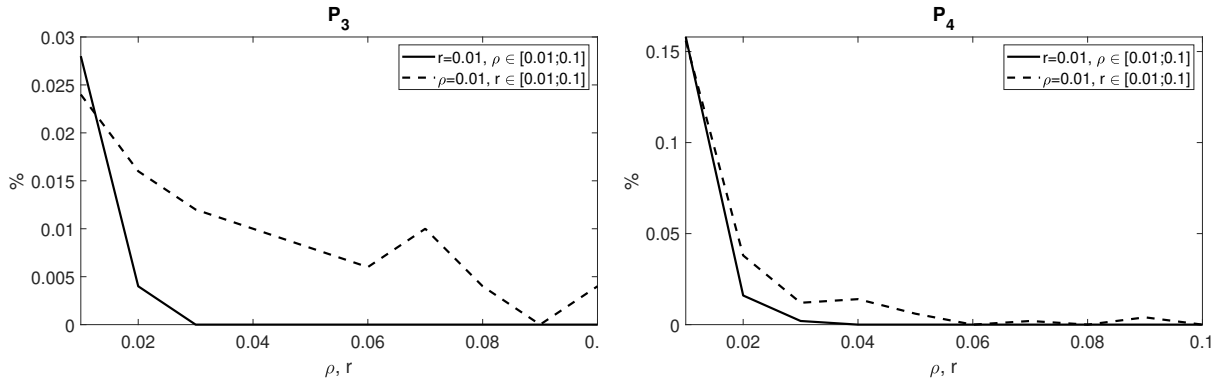

Figure 23: Number of simulated outputs outside estimated bounds LSUO (left) and LSUP (right) for system S_3 (48) depending on state noise parameter ρ and output noise parameter r.

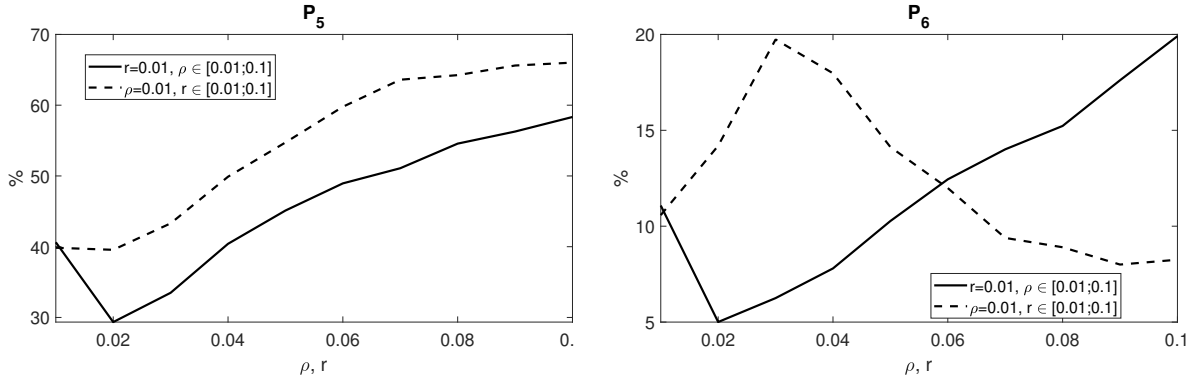

Figure 24: number of state (left) and predictive (right) pdf support volumes (LSUP) smaller than corresponding support volumes (LSUO) for system S_3 (48) depending on state noise parameter ρ and output noise parameter r.

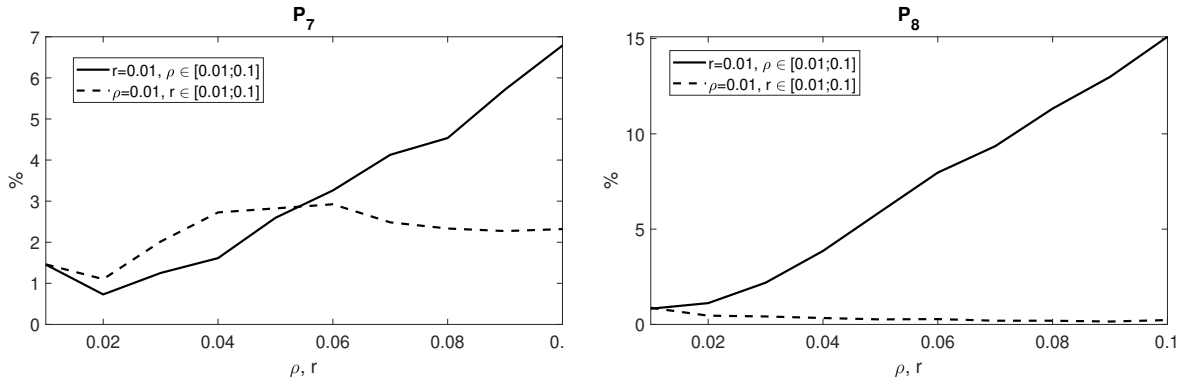

Figure 25: Number of state (left) and predictive (right) pdf supports (LSUP) fully nested inside corresponding supports (LSUO) for system S_3 (48) depending on state noise parameter ρ and output noise parameter r.

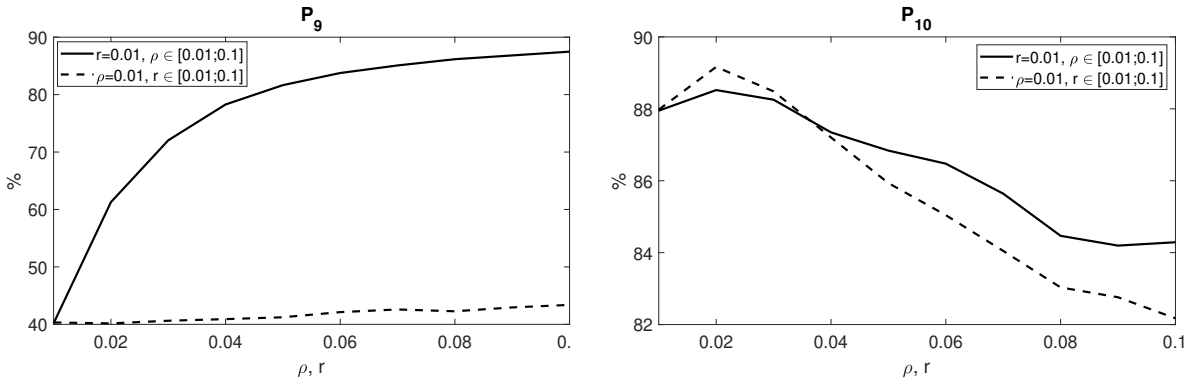

Figure 26: Average percentage of state (left) and predictive (right) pdf support (LSUP) lying inside corresponding support (LSUO) for system S_3 (48) depending on state noise parameter ρ and output noise parameter r.

4.5 Discussion

Results for system S_1 show that the TNSE of states estimation using algorithm LSUO (criterion T_1) increases with increasing uncertainty. The influence of the state noise parameter ρ is more significant than of the parameter r. Similar trend is observed in the results for system S_3. On the other hand, in system S_2 the results of T_1 are different. Increasing state uncertainty does not influence the value of TNSE. Its value is influenced only by increasing output noise.

The algorithm LSUP for system S_2 performs very similar to the LSUO algorithm in the state estimation. Although the TNSE of LSUP (T_2) shows slightly lower values, the results and dependencies are almost the same. For system S_3 results for criteria T_1 and T_2 show the same dependencies but the absolute TNSE values are higher for the LSUP algorithm.

Comparing the TNSE of output prediction using LSUO (T_3) and LSUP (T_4) for system S_3, we can see that the values differ very mildly. The trend for both is that the value of TNSE is influenced by rising uncertainty of both parameters ρ and r. For system S_2 the algorithm LSUP performers significantly better then LSUO in the sense of lover TNSE of output prediction. The results for rising state uncertainty show about hundred times higher value of TNSE of output prediction using LSUO algorithm then using algorithm LSUP. In system S_1 the situation is reversed. The LSUO performs approximately hundred times better than LSUP in output prediction in the sense of TNSE.

Independently of used system, the state bounds estimated by algorithm LSUO show higher success in containing the actual states. This can be caused by the fact that in general the pdf supports approximated by LSUO algorithm are bigger in volume. The volume comparison shows criterion P_5. Especially for systems S_1 and S_2 the vast majority of volumes on LSUO is bigger than in LSUP. The volume of state support pdf is depicted on graphs (3), (12) and (20). In figure (3) the difference between algorithms is obvious. Parallelotopic supports are approximately thousand times smaller in volume than corresponding orthotopic supports. Eventhought, for systems S_2 and S_3 the difference in volumes is not that striking, the parallelotopes are generally smaller as well. The contrast of volumes explains the higher success of LSUO in containing the actual states inside predicted bounds. Reduction of the pdf support volume in LSUP implicates partial information loss.

Both algorithms perform better in predicting output bounds than in estimating state bounds. For all systems the LSUO algorithm reports less actual outputs outside predicted bounds. The output is scalar hence its predictive pdf is an interval. For the length comparison the criterion P_6 was introduced. For system S_2 the absolute majority of supports predicted by LSUO is longer. Figures (4) (13) and (21) show the absolute values of predictor support length. For system S_2 the LSUP predictor supports are hundred times smaller.

For further analysis of the relationship between the supports of pdfs approximated by algorithms LSUO and LSUP we explore the number of pdf supports of LSUP fully nested inside corresponding pdf supports of LSUO (P_7 and P_6). In systems S_1 and S_2 is the number of fully nested state supports generally slightly higher than predictive pdf supports. In system S_3 the situation is reversed. Although the differences are very low, in system S_2 the nesting probability shows higher dependence on the output noise parameter r.

The figures (9), (17) and (26) demonstrate the results of overlap analysis of the geometrical objects

(orthotopes and parallelotopes) used for pdf approximation. The numbers are significantly higher than criteria P_7 and P_8. This indicates that the objects overleap in majority of its volumes. The reason why many parallelotopes are not fully nested inside corresponding orthotopes could be found in the approximation process of pdf supports described earlier. The geometrical approach from [9] which was used for approximating zonotopes by parallelotopes can shift the resulting parallelotope.

Even though exceptions can be found, the performance of both algorithms show higher dependence on the state noise parameter ρ. Despite the fact that the LSUO algorithm shows generally lower TNSE for state estimation as for output prediction and predicted bounds often contain the actual states and outputs, the LSUP algorithm successfully reduces the area of uncertainty which is evident from the volume comparison.

5 Conclusions

In this paper, two algorithms for estimation of unknown states and output prediction were described and compared. Both algorithms for Bayesian state estimation and output prediction using state space model with uniform noise are based on an approximation of the state pdf after time update and data update and predictive pdf. The difference between the two is that in LSUO in each step the complex exact pdf after time update and data update and predictive pdf are approximated by uniform pdfs on orthotopic support. In LSUP algorithm are the pdfs approximated by a uniform pdfs on parallelotopic support. The approximations prevent increasing complexity of computation and keeps the pdfs in the given class.

The results of this report together with results presented in [3] will be used in the research concerning the knowledge transfer between uniformly modelled Bayesian filters. The recent paper [5] solves this problem using the LSUO algoritm. The using of LSUP algorithm promises a better performance as presented in the submission [4]. Nevertheless, a more detailed analysis is needed to confirm this hypothesis.

References

[1] E. Gover and N. Krikorian. Determinants and the volumes of parallelotopes and zonotopes. In *Linear Algebra and its Applications*, pages 28–40. 443(1), 2010.

[2] L. Jirsa, L. Kuklišová Pavelková, and A. Quinn. Approximate Bayesian prediction using state space model with uniform noise. In *Informatics in Control Automation and Robotics*, volume 613 of *Lecture Notes in Electrical Engineering*, pages 552–568. Springer International Publishing, Cham, 2020.

[3] L. Jirsa, L. Kuklišová Pavelková, and A. Quinn. Bayesian filtering for states uniformly distributed on a parallelotopic support. In *2019 IEEE International Symposium on Signal Processing and Information Technology (ISSPIT 2019)*, Ajman, United Arab Emirates, December 2019.

[4] L. Jirsa, L. Pavelková, and A. Quinn. Bayesian transfer learning between uniformly modelled bayesian filters. In Oleg Gusikhin and Kurosh Madani, editors, *Informatics in Control Automation and Robotics*, Lecture Notes in Electrical Engineering. Springer. Submitted.

[5] L. Jirsa, L. Kuklišová Pavelková, and A. Quinn. Knowledge transfer in a pair of uniformly modelled bayesian filters. In *Proc. of the 16th Int. Conf. on Informatics in Control, Automation and Robotics (ICINCO 2019)*, volume 1, pages 499–506, Prague, Czech republic, 2019.

[6] J. Lawrence. Polytope volume computation. In *Mathematics of Computation*, volume 57, pages 259–271. 1991.

[7] L. Pavelková and K. Belda. State estimation and model predictive control for the systems with uniform noise. In *Proc. of 11th IFAC Symposium on Dynamics and Control of Process Systems, including Biosystems (DYCOPS-CAB 2016)*, pages 967–972, 2016.

[8] L. Pavelková and L. Jirsa. Approximate recursive Bayesian estimation of state space model with uniform noise. In *Proc. of the 15th Int. Conf. on Informatics in Control, Automation and Robotics (ICINCO 2018)*, pages 388–394. Porto, Portugal, 2018.

[9] A. Vicino and G. Zappa. Sequential approximation of feasible parameter sets for identification with set membership uncertainty. In *IEEE Transactions on Automatic Control*, volume 41(6), pages 774–785. 1996.